Hindawi
Journal of Electrical and Computer Engineering
Volume 2022, Article ID 3074298, 12 pages
https://doi.org/10.1155/2022/3074298

Research Article

Improvement of the Resilience of a Microgrid Using Fragility Modeling and Simulation

Santhan Kumar Ch,[1] N. Karuppiah,[2] B. Praveen Kumar ,[2] S. Shitharth ,[3] and B. Dasu[4]

[1]*Department of EEE, Lords Institute of Engineering and Technology, Hyderabad, India*
[2]*Department of EEE, Vardhaman College of Engineering, Hyderabad, India*
[3]*Department of CSE, Kebri Dehar University, Somali, Ethiopia*
[4]*Department of EEE, Gudlavalleru Engineering College, Vijayawada, India*

Correspondence should be addressed to S. Shitharth; shitharths@kdu.edu.et

Received 4 March 2022; Revised 21 July 2022; Accepted 30 July 2022; Published 24 August 2022

Academic Editor: Ahmed A. Zaki Diab

Copyright © 2022 Santhan Kumar Ch et al. This is an open access article distributed under the Creative Commons Attribution License, which permits unrestricted use, distribution, and reproduction in any medium, provided the original work is properly cited.

The modern microgrid is designed to withstand various disruptive events that have a high probability of occurrence but have a low impact on the system. This improves the reliability of the system but does not take into consideration the disruptive events that have a low probability of occurrence but have a large impact on the system, such as extreme weather or natural disasters. Redesigning a microgrid to withstand low probability high impact events is very costly and is not a feasible solution to existing microgrids. This paper proposes a method to improve the resilience of an existing microgrid to quickly recover from low probability high impact events. The method used for this purpose is a combination of Monte Carlo simulation and prioritization of load of the microgrid. The efficacy of the method is examined by modeling microgrids using a fragility model. Using the proposed novel resilience index, the resilience of the IEEE 5-Bus system and IEEE 14-Bus system and the effect of load shedding on the resilience of the microgrid are analyzed and presented. The effect on smaller and larger grids and their resilience is examined. A novel resilience index is used to quantify the improvement of resilience of the proposed method when compared to other methods available in the literature.

1. Introduction

Power system resilience is defined as the capability of the power system to withstand and recover from any disturbance. With the use of modern controllers and advanced automatic control systems, the power system is able to withstand and recover from a wide variety of disturbances. This is due to the fact that the power system and control system are generally designed by taking the major disturbances into consideration and have been optimized to either automatically clear the disturbance or work around the disturbance without disrupting power supply to the consumers. This is achieved using the implementation of additional components to the power system to increase redundancy. This increases the reliability and resilience of the system. To optimize the increase in reliability, the major disturbances are selected to be modeled and analyzed based on a few criteria. A few prominent criteria are the frequency of the disturbance or probability of occurrence of the disturbance, the impact of the disturbance on the system or consumer, and the cost of implementing a solution to the disturbance. This increases the system's resilience to high-impact high-frequency events, such as lightning strikes, variation in load, etc., and low-impact high-frequency events, such as faults and fluctuations, etc. Low-impact low probability events are generally ignored at this stage and are dealt with as and when they occur on a case-by-case basis. This leaves the system vulnerable to high-impact low-frequency events, such as extreme weather conditions, natural disasters, cyberphysical attacks, geomagnetic storms, electromagnetic pulses, etc.

Microgrids are low voltage or consumer end systems with Distributed Energy Resources (DERs) together with storage devices and flexible loads. DERs include

microturbines, fuel cells, Photo Voltaic systems, etc., either singularly or a combination of them. Storage devices used may be flywheels, energy capacitors, batteries, or a combination of them. Such microgrids can be operated autonomously without connection to the power grid, i.e., in islanded mode or connected to work along with the grid connection. The operation of a microgrid in the distribution network provides immense benefits to the overall performance of the distribution system if it is efficiently controlled and coordinated. They usually cover only a small area of the overall network. In the event of an emergency or a failure of the system, the distribution network can be maintained by dividing into clusters of microgrids. The latest designs of distribution networks all include optimally placed DERs in the network for ease of division of the network into microgrids in the event of grid failure to provide uninterrupted power to the consumers. Microgrids tend to increase the complexity of the control system required to regulate the power distribution system while connected to the grid but require only simple control systems if run in islanded mode.

In [1], it is indicated that although extreme weather phenomena, such as cyclones, landslides, etc., have a low probability of occurrence, it is predicted that such events may increase in severity and probability in the future, and the power system must be made resilient to them in response. This calls for a major overhaul of the existing power system and redesigning it to be resilient against such extreme weather events using hardened infrastructure and redundant supply.

This is a very costly affair in both resources required, and research effort such as hardening the system to a great degree increases the brittleness of the system; i.e., the system will withstand a lot of disturbances, but if and when it fails, it becomes irreparably damaged and will have to be completely replaced. Extensive research will have to be done to determine the optimal hardness of the system without making it too brittle.

This affects different parts of the transmission network differently. On the high voltage side, such measures are very crucial and have already been implemented using superior transmission tower designs, wider spacing between the conductors, sturdy anchoring, and an increase in periodic maintenance. This is due to the high level of redundancy already available in high voltage networks over long distances; i.e., they are highly interconnected, and thus, they can be easily scheduled to be switched off and maintained or replaced. This mitigates the impact of extreme weather events at a high voltage level.

This is not true for the low voltage level of power distribution as the level of redundancy is not as high as that of the high voltage system. There is very limited space to increase the gap between conductors in residential areas to mitigate the effect of high wind speeds. There are also restrictions due to the proximity of existing residential complexes or apartments. This issue can be avoided by including these factors during the design of a new distribution area or residential area, but it is not feasible for existing networks as the process of implementing the recommended changes to the network is very cost-prohibitive. It is necessary to improve the resilience of the low voltage distribution systems, such as microgrids against extreme weather.

In the search for existing research on the topic of improvement of power system resilience, the resulting papers have been analyzed based on three key attributes. These attributes are not exhaustive and do not extend to all the papers researched. The attributes are as follows: problem solved, the method of the solution implemented, and test cases used. While almost all of them comment on the effect of severe weather on the power system, they approach the problem in different ways. Panteli et al. [1] used fragility curves to assess the impact of extreme weather on a simplified 29-bus Great Britain transmission network. Panteli et al. [2] used defensive islanding to improve resilience on the simplified 29-bus network. The improvement of the system function in zones 2,3 and 4 was observed due to this strategy. Najafi et al. [3] used a social welfare-based index and genetic algorithm to improve resilience on an IEEE 33 node system. The targeted improvement of the system in zone 4 in sync with the codependent water system greatly enhanced the resilience of the system in accordance with the demand. Gao et al. [4] used Linear Integer Programming (LIP) to emulate all feasible paths of restoration of the system to determine the optimal restoration of critical loads on an IEEE 123 node feeder system. The targeted improvement of the system resilience in zone 4 was highly cost-effective. Xu et al. [5] also used LIP to restore critical loads on the microgrids of the distribution system of Pullman, Washington and were focused on the improvement in zone 4 of the system resilience. Ma et al. [6] used the greedy search algorithm to minimize the cost of hardening of system and load shedding to improve resilience in a modified Electric Power Research Institute (EPRI) test circuit. The improvement to both zone 2 and zone 4 was significant. Farzin et al. [7] used Mixed Integer Linear Programming (MILP) to enable the smart distribution of resources in a three microgrid test system to improve resilience. The research was targeted toward improvement in zones 3 and 4 while minimizing the cost of the improvement. Bajpai et al. [8] used Graph theory and Choquet Integral to maintain critical load supply in IEEE 123 node distribution system. The target was to reduce the impact on zone 2 and increase the recovery in zone 4. Li et al. [9] used a combination of fragility curves and the Monte Carlo method to determine the optimal location for the integration of DERs in an IEEE 37 bus network. The target was to improve the resilience in zone 1 and reduce impact in zone 2. Huang et al. [10] used a nested column-and-constraint generation decomposition, generator redispatch, topology shifting, and load shedding to improve the resilience of a modified PJM 5 bus system, IEEE one area RTS-96 system, and IEEE three area RTS-96 system. The improvement was observed in zones 1, 2, 3, and 4. Zarre-Bahramabadi et al. [11] used MILP optimization to determine the optimal placement of switches to improve the resilience of Bus 4 of the Roy Billinton test system. Zones 1 and 2 showed improvement due to this method. Mousavizadeh et al. [12] used MILP to analyze the resilience of a modified 118 bus test system and one 20 kV distribution

network in Tehran, Iran. Gholami et al. [13] observed the working of a resilient microgrid using a two-stage stochastic programming approach and its ability to reduce the impact of electric interruption by using the microgrid capabilities of the IEEE 33-bus test system used. Eshghi et al. [14] proposed metrics for the grading or ranking of optimal operation of a smart grid using state estimation and adaptive response techniques and their advantages. Chanda and Srivastava [15] used percolation theory and a hierarchical analytical process to define and quantify the resilience of an electrical distribution system with multiple microgrids. Panteli et al. [16] used time-dependent resilience metrics to quantify and analyze the different phases that a power system may experience during an extreme event of the 29-bus Great Britain transmission network. Panteli et al. [17] gave a comprehensive understanding of the use of hardening and implementation of smart control as strategies to improve resilience on the 29-bus Great Britain transmission network. Xu et al. [18] used a look-ahead load restoration strategy to determine the optimal restoration strategy to improve the resilience in zone 4 of the modified IEEE 342-node low voltage network. Singaravelan and Kowsalya [19] used load shedding and fuzzy logic techniques to prolong the supply of power to the islanded microgrids of a modified IEEE 34-node sample system and thus improved the resilience in zones 2 and 3 of the network. Nikmehr et al. [20] used metaheuristic algorithms under the condition of uncertainties of loads and DERs to determine the optimal scheduling of generators on a microgrid-based smart grid. Chen et al. [21] used a sequential service restoration framework and MILP techniques to optimally integrate smart grids, such as a modified IEEE 123-node test feeder. Ji et al. [22] used Soft Open Point (SOP) and MILP techniques to improve load recovery and increase the resilience in zones 4 and 5 of the IEEE 33-node and IEEE 123-node test feeders. Chanda et al. [23] used and evaluated a dynamic optimization algorithm to change the operating criteria to increase the ability of the two connected CERTS microgrids to ensure quality supply to the most critical loads of the system. Chen et al. [24] used MILP, remote-operated switches, and DERs to restore critical loads of a modified IEEE distribution rest system and increase resilience in zone 4 of the system. Panteli and Mancarella [25] used a sequential Monte Carlo-based time-series simulation and fragility curves to improve the resilience of an IEEE 6-bus test system in order to reduce the impact of severe weather on the system. Gholami and Aminifar [26], MILP, and Benders' decomposition techniques were used to facilitate restoration, reduce outage duration, and reduce damage to critical system components of an IEEE 39-bus system to increase resilience in zones 1, 2, 3, and 4 of the system. Reed et al. [27] used fragility, outage restoration, and interdependency analysis techniques to understand and quantify the behavior and resilience of the system using data collected during Hurricane Katrina. Arab et al. [28] used MILP and Benders' decomposition algorithm to determine the optimal repair schedule, generator commitment, and network configuration of an IEEE 118-bus test system to increase its resilience to disasters and improve resilience in zones 1, 2, 3, and 4 of the system. Eder-Neuhauser et al. [29] used the implementation of a decentralized and self-organizing structure to qualitatively evaluate the resilience and security of a smart grid with an Information and Communication Technology (ICT) topology. Eskandarpour and Khodaei [30] used machine learning-based outage prediction to determine the potential outage of the power grid components in a hurricane. Liang et al. [31] used the control of Electric Springs implemented in a microgrid with ES Topology to enhance the resilience of microgrids using frequency and voltage control. Liu et al. [32] used a four-loop switching controller implemented in a modified IEEE 16-generator 68-bus power system to improve the transient stability of power systems with wind power integration. Liu et al.[33] used the Monte Carlo method to improve the resilience of IEEE 30-bus and 118-bus systems by determining the optimal microgrid clustering of the system and also studied [34]. An optimal active power dispatch can also be done by using deep reinforcement learning [35].

Ali et al. [36–38] discussed the optimal planning of autonomous microgrids in the presence of uncertain PV and wind generation units, PEV charging stations/parking lots, and proposed a bilevel metaheuristic and a two-level multiobjective evolutionary algorithm-based solution to address the complex planning model.

From the literature, it is made clear there is a need to develop a methodology to address and study the resilience of a microgrid subjected disrupting events having a larger impact on the microgrid. In this work, it is proposed to use a combination of Monte Carlo simulation and load shedding to improve the resilience of the power system. Monte Carlo simulation is used to simulate the effect of wind on the system using random variables with normal distribution and the effect of load shedding on the resilience of the system.

The rest of the paper is organized as follows. Section 2 presents the fragility modeling, the resilience of the power system, and possible strategies to improve resilience. Section 3 presents the overview of the simulation, test models of the power system used, a brief overview of the Monte Carlo simulation method and load shedding algorithm used, the overall simulation flowchart, and the results obtained from the simulation. Section 4 summarizes and concludes the paper.

2. Fragility Modeling and Resilience Assessment

2.1. Fragility. Fragility is the probability of failure of a structure based on a specific parameter. In a system, the probability of failure depends on the fragility of the weakest or the most vulnerable component in the system. This depends heavily on the intensity of the parameter in question. A fragility function is a mathematical relation between the failure probability of a component and the specific parameter intensity acting on or experienced by the component either directly or indirectly. For example, the fragility function of a transmission pole depends on the intensity of the shaking of the ground in an earthquake or the force experienced by the transmission pole due to the high-speed spiraling wind blowing on it in a cyclone. Figure 1 shows the

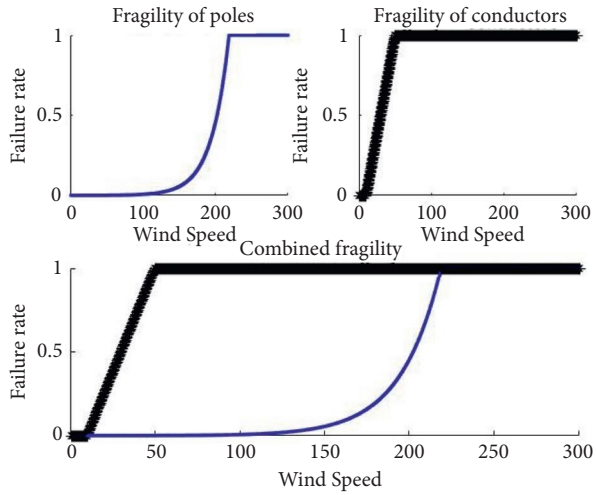

Figure 1: Fragility curves of transmission poles and conductors w.r.t wind speed.

fragility curves for transmission lines subjected fragility of poles, conductors, and combinations. From the figure, it is clear that poles are impacted at higher wind speeds, and conductors have an adverse impact even at lower wind speeds, and it is also shown the combined fragility of the system.

2.2. Resilience. The ability of the system, including generating sources, transmission, and distribution, to bounce back from high-impact low-frequency events is called resilience. This could include events that are natural, such as cyclones, earthquakes, or ice storms, etc., as well as man-made, such as cyber or physical attacks on grid infrastructure. The system is represented by a system function F(t) which indicates the state of the system at a time *t,* as illustrated in Figure 2.

2.2.1. Zone 1 (Normal State). This represents the state of the system before the disruption event. This is the designed state of the system. The system will continue to be in this state until there is a disruption to the system.

2.2.2. Zone 2 (Disruption State). This represents the state of the system after the disruption until the failure of the system. The system function falls due to either the failure of system components or due to preventive measures programmed into the system in response to specific stimuli. The degree of fall in the system function depends upon the severity of the disruption and the preventive measures taken by the implemented control system.

2.2.3. Zone 3 (Fail State). This represents the state of the system after the failure of the system until the recovery of the system is attempted. The system function stays in this state until the repair or replacement of damaged components of the system after the disruption event is over. The duration of this state depends upon the severity of the disruption event and its duration.

2.2.4. Zone 4 (Restoration State). This represents the state of the system after the attempted recovery starts until the system reaches the recovered state. In this state, the power system undergoes repair or replacement of damaged components of the system. The level of recovery of the system function and the rate of recovery depends on factors such as the measures taken by the system operator, the resilience of the system, etc.

2.2.5. Zone 5 (Recovery State). This represents the state of the system after the system reaches the recovered state. The system continues to be in this state until there is another disruption or heavy repairs or replacement of damaged components due to the disruption. This state does not change until there is a change in the structure of the power system.

2.3. Possible Solutions. There are a wide variety of strategies that can be implemented to improve the resilience of a system. These strategies can either be individually implemented or implemented together in a group. The strategy to be implemented depends upon the zone of the resilience of the system to be targeted for improvement. A few strategies categorized by their targeted zone of improvement are as follows.

2.3.1. Zone 1 Improvement. In this zone, the goal of improvement is to prevent damage to the system. This can be achieved by predicting the occurrence of the disruption by analyzing previous disruptions, determination of weak points in the system, analysis of the cause of the disruption, and forecasting the conditions in which the disruption occurs. These strategies work well with the strategies implemented in zones 2 and 5.

2.3.2. Zone 2 Improvement. In this zone, the goal of improvement is to reduce the severity of the impact of the disruption or reduction in the rate of degradation of the system, or both. This can be achieved by hardening of the most vulnerable power system components, increasing the level of redundancy in the system. These strategies work well with the strategies implemented in zones 1 and 3.

2.3.3. Zone 3 Improvement. In this zone, the goal of improvement is to reduce the duration of the failed state. This can be achieved by implementing backup reserves, optimal placement of service centers in an area, and improving identification of the location of the damaged components of the system. These strategies work well with the strategies implemented in zones 2 and 4.

2.3.4. Zone 4 Improvement. In this zone, the goal of improvement is to increase the rate of recovery of the system or improve the level of recovery, or both. This can be achieved by implementing load shedding, prioritization of load, installation of optimally placed DERs, and optimal clustering

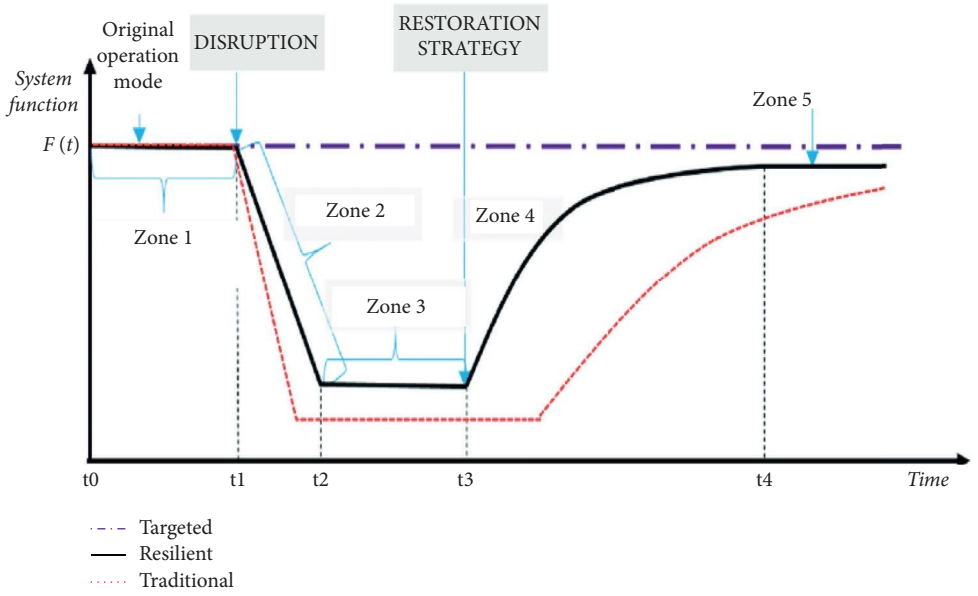

Figure 2: Representation of system resilience.

of microgrids. These strategies work well with the strategies implemented in zones 3 and 5.

2.3.5. Zone 5 Improvement. In this zone, the goal of improvement is to maintain the new stable state of the system and bring the system back to its original state. This can be achieved by a restructuring of the system, replacement of damaged components, analysis of the effect of the disruption, and archiving of the same for future use, etc. These strategies work well with the strategies implemented in zones 4 and 1.

2.4. Proposed Index. It is observed that after the Monte Carlo simulation, we can find the average power generated by a bus in all the scenarios run by the simulation. The probability of being in a specific state of the power generation in each bus is determined by counting the number of occurrences divided by the number of simulations. The Average Total Power Generated (ATPG) and the Average Total Power Consumed (ATPC) at each bus are also determined from the simulation data as follows:

$$\text{ATPG} = \frac{\sum_{i=1}^{\text{iter}} \text{TPG}(i)}{\text{iter}}, \tag{1}$$

where iter is the total no. of iterations of the Monte Carlo simulation, TPG(i) is the Total Power Generated in ith iteration of the Monte Carlo simulation as follows:

$$\text{ATPG} = \frac{\sum_{i=1}^{\text{iter}} \text{TPC}(i)}{\text{iter}}, \tag{2}$$

where iter is the total no. of iterations of the Monte Carlo simulation, TPC(i) is the total power consumed in ith iteration of the Monte Carlo simulation as follows:

$$\begin{aligned} P_G &= \frac{\text{ATPG}}{\text{Total base power generated}}, \\ L_s &= \frac{(\text{ATPC} - \text{Total base power consumed})}{\text{Total base power consumed}} * 100, \\ \text{resilience index}\,(RI) &= (a * P_G) + (b * L_s), \end{aligned} \tag{3}$$

where a and b are coefficients assigned to the system as follows:

$$\begin{aligned} a &= \frac{1}{\text{no of buses in the system}}, \\ b &= \frac{1}{\text{no of loads in the system}}. \end{aligned} \tag{4}$$

3. Modeling and Simulation

The probability of failure of the power system components is determined by using the fragility function with wind speed as input and the probability of failure as the output. It is determined to use the fragility curve of a power line as it is the most sensitive to wind speed. In this case, the conductors are the weakest link in the power system distribution chain and are most likely to be a point of failure due to the pressure caused by the wind [3]. Therefore, the equation for the fragility of a conductor becomes as follows:

$$\begin{aligned} \text{pfc} &= 0 \,\forall\, w_s \langle w_{\min}, \\ \text{pfc} &= \frac{(w_s - w_{\min})}{(w_{\max} - w_s)} \,\forall\, w_{\min} \le w_s \le w_{\max}, \\ \text{pfc} &= 1 \,\forall\, w_s \rangle w_{\max}, \end{aligned} \tag{5}$$

where pfc is the probability of failure of a conductor, w_s is the speed of the wind in the local area, $w_{\min}$ is the minimum

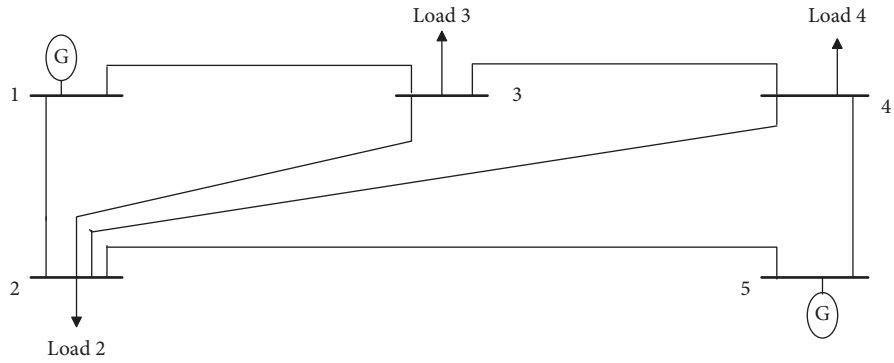

Figure 3: Single line diagram of an IEEE 5-bus System.

wind speed required for failure below which the conductor does not fail due to the wind, and w_{max} is the maximum wind speed above which the conductor is sure to fail.

3.1. Systems Studied. The models used for simulation are as follows, IEEE 5-Bus system depicted in Figure 3, is used for simulation of the power system consisting of five buses and seven lines. IEEE 5-Bus system depicted in Figure 4 is used for simulating power system configuration, which consists of 14 buses and 20 lines.

The simulation and implementation of the solution to the test cases in consideration would be meaningless without comparison with base steady-state data obtained using power flow equations. Of the wide variety of power flow equations available to determine the flow of power in the system at a steady state, a few are the Gauss-Seidel method, Newton-Raphson method (NR method), fast decoupled load flow method, DC load flow method, etc. Each method has its own advantages and disadvantages based on the assumptions made in the calculation of the power flow. Of these, we use NR load flow to determine an accurate load flow with a very small number of steps. The disadvantage of longer calculation time and larger memory requirement of NR load flow method is overcome by the speed and capability of the latest computers and also the vast boost to computing power afforded by graphical processing units (GPUs) that perform a large number of calculations simultaneously.

3.2. Monte Carlo Simulation. It is one of the deterministic approaches to the solution of a problem in which multiple random variables are used to make numerical estimations of complex situations. It is generally used to calculate the impact of a parameter on the system by running a large number of iterations of the simulation of the system in which the parameter in question is slightly different in value or completely random based on a selected random distribution. It gives us the probability of the system being in a certain state by adding up the number of times the target state is achieved during the course of the Monte Carlo simulation. The selection of the type of random distribution is decided based on the parameter in question and its behavioral tendencies. Generally, the random number is chosen to be with a uniform distribution where all possible values within

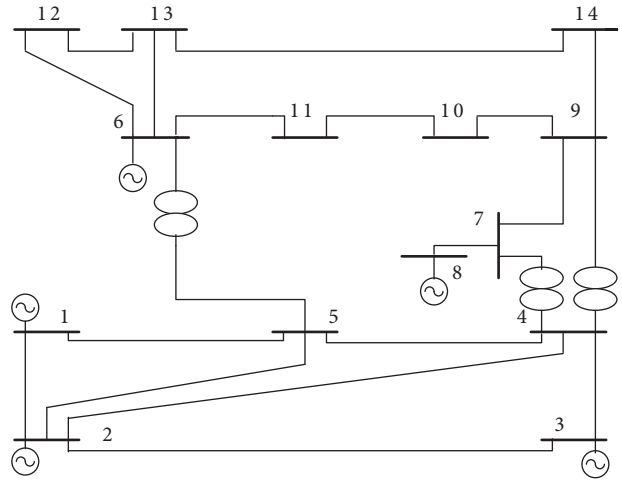

Figure 4: Single line diagram of an IEEE 14-bus System.

a range are equally probable, or it is chosen to be with normal distribution to emulate the probabilities found naturally in nature.

The Monte Carlo simulation technique is used to emulate the effect of high-speed wind on the test system by the use of a normally distributed random number to represent the wind speed and comparison with the reduced fragility function adjusted to the natural tendency of wind to determine the failure state of the transmission line in question and its effect on the system. Since the goal is to quantize the resilience of the system, the state of the system is observed using specifically designed indices. In this case, the total power generated, the total load supplied, the ratio of power generated to the power consumed, etc. The end goal is to maximize the total load supplied while minimizing the total generation shift during a failure.

3.3. Load Shedding. It is not always possible to satisfy all the loads in a system during a breakdown of one of its components. In such cases, load shedding is one of the solutions implemented to temporarily reduce the demand on the system to a more manageable state depending upon the generating capability of the system.

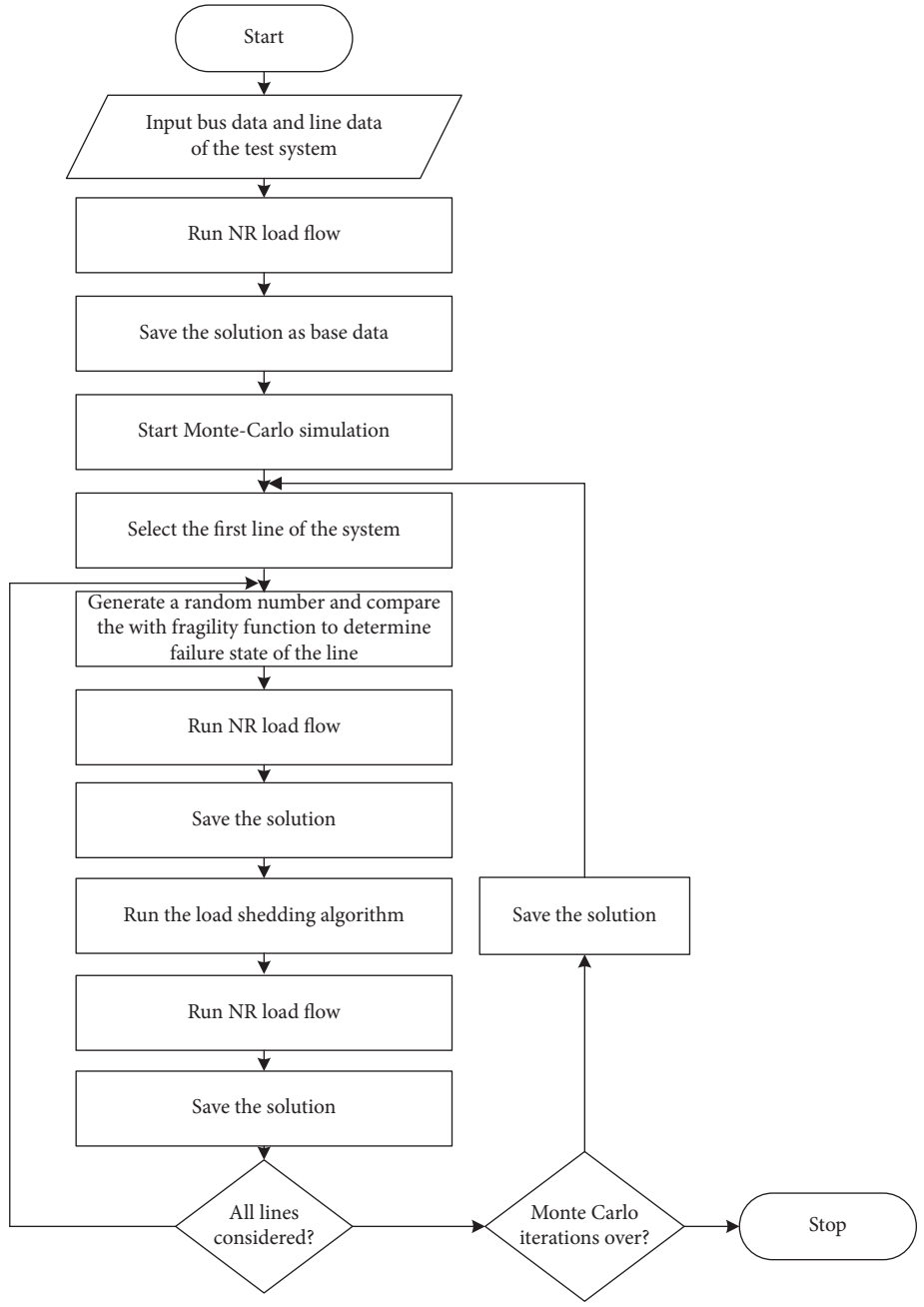

Figure 5: Flowchart representation of the simulation.

The process of load shedding is traditionally done by either completely dropping the smallest noncritical load or reducing the highest noncritical load by a nominal amount. There are large variations of this method available for use based on the demand and individual requirements. Critical loads are always a priority and are to be supplied at any cost, even if all the noncritical loads must be shed to do so. Only in the event of a risk of a hazard is a critical load to be shed. In extreme conditions where power grid supply is not available, and the installed DERs in the network do not have enough capacity to supply the demands of the islanded microgrid network, load shedding is the last hope for the continuation of supply after all other methods fail.

In the case of the current experiment, the Monte Carlo simulation is run both with and without load shedding to compare both strategies and their effect on resilience by comparison of the resilience indices.

3.4. Simulation Flowchart. The simulation flowchart is shown in Figure 5.

3.5. Result. Upon Monte Carlo simulation of the test systems, we obtain the probability distribution of the power generated at each bus of the system. The cumulative power distribution curve gives the cumulative probability of the

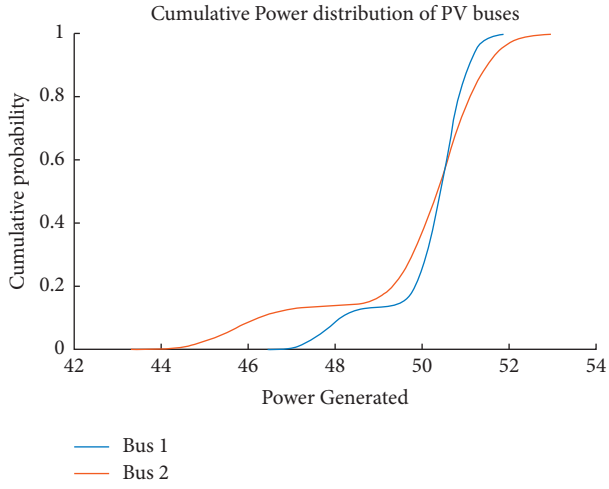

Figure 6: Cumulative power distribution at buses 1 and 2.

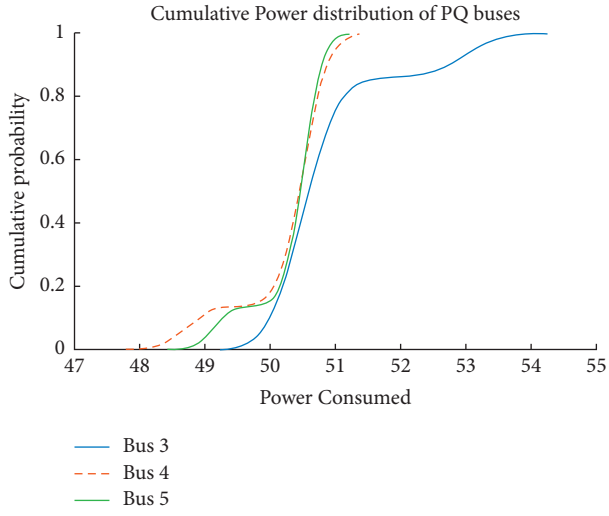

Figure 7: Cumulative power distribution at buses 3–5.

power et al. values of power. The most probable power magnitude is obtained by identifying the largest change in the cumulative probability within the neighborhood of the tolerance of the power value. The probability density curve gives the density of probability of the value of power. The probability of a specific power magnitude is the area under the curve around the neighborhood of the power value. The commutative power distribution for PV and PQ buses (buses 1–5) before load shedding for the IEEE-5 bus system is shown in Figures 6 and 7.

For the IEEE 5-Bus system without load shedding, the total power generated was found to be 234.3689 MW compared to the base power generation of 21.4769 MW. While total power consumed was found to be 1.2235 MW compared to base power consumed at 1.699 MW. The weights $a = 1/5$ and $b = 1/3$.

Therefore, $L_S = 27.98$, $P_G = 10.91$, and RI = 11.50.

The power density distribution for buses 1,2, and buses 3,4, and 5 before load shedding for the IEEE-5 bus system are

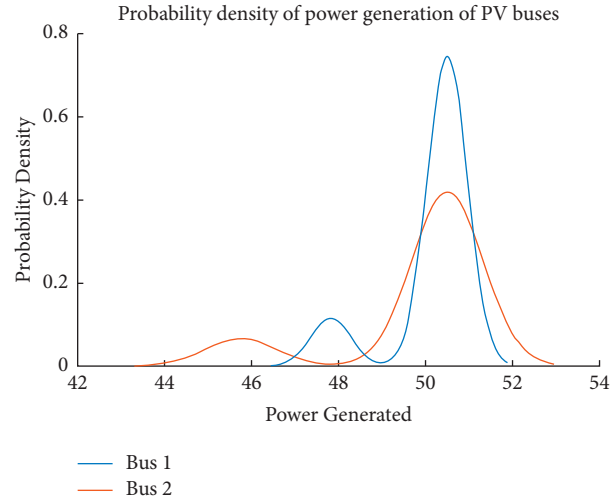

Figure 8: Power density distribution at buses 1 and 2.

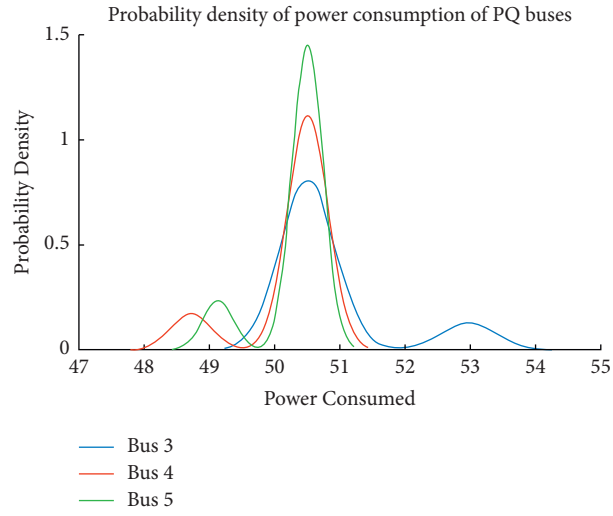

Figure 9: Power density distribution at buses 3–5.

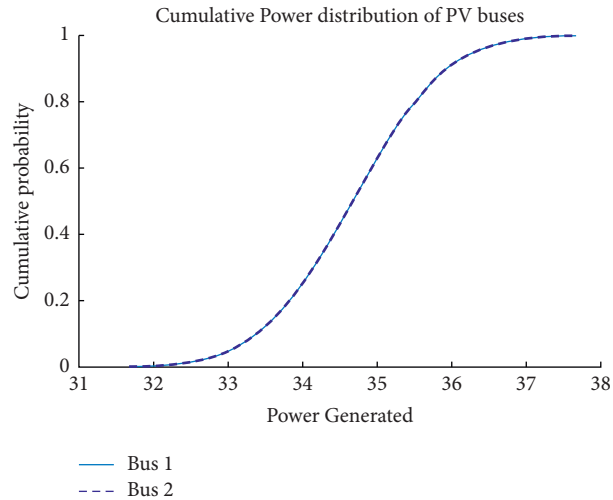

Figure 10: Cumulative power distribution at buses 1 and 2.

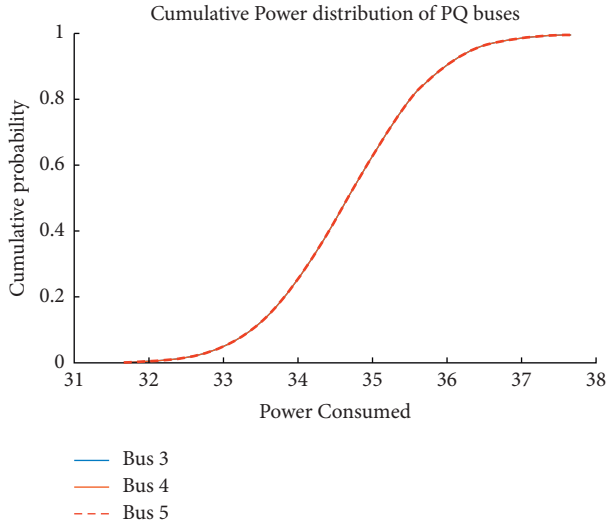

Figure 11: Cumulative power distribution at buses 3–5.

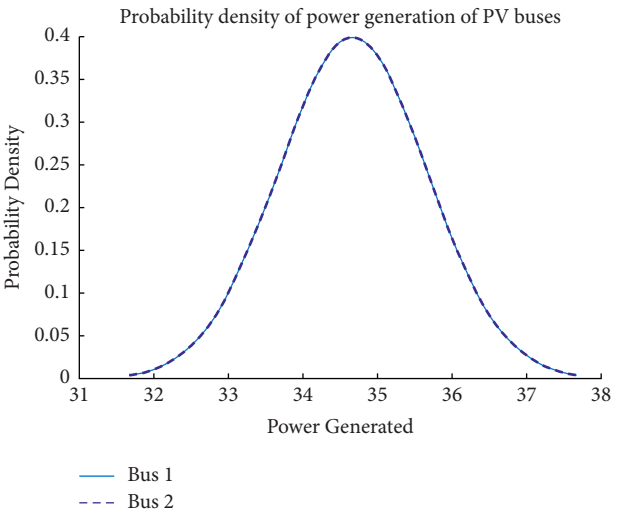

Figure 12: Power density distribution at buses 1 and 2.

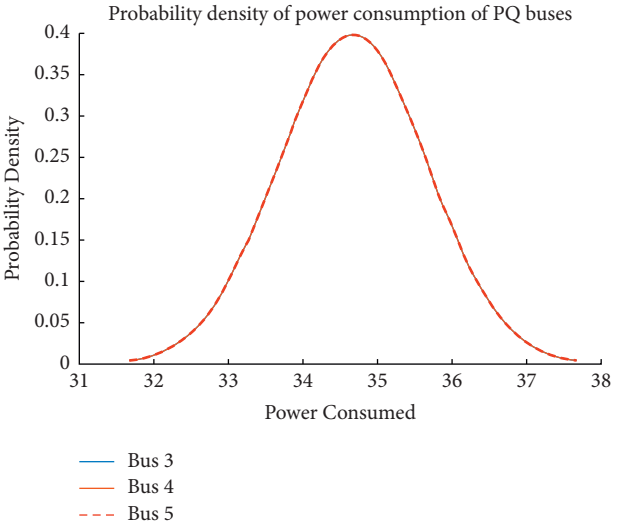

Figure 13: Power density distribution at buses 3–5.

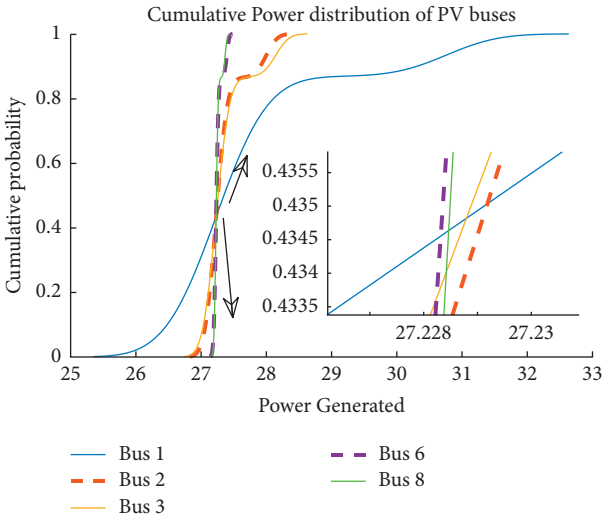

Figure 14: Cumulative power distribution at buses 1, 2, 3, 6, and 8.

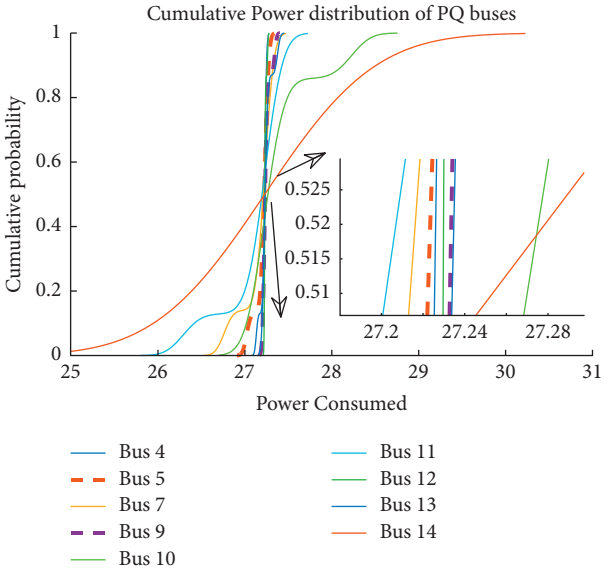

Figure 15: Cumulative power distribution at buses 4, 5, 7, and 9–14.

shown in Figures 8 and 9. Figure 8 shows the slack and generator buses, and Figure 9 shows for load buses.

The commutative power distribution for PV and PQ buses (buses 1–5) after load shedding for the IEEE-5 bus system is shown in Figures 10 and 11.

For the IEEE 5-Bus system with load shedding, the total power generated was found to be 172.8266 MW compared to the base power generation of 21.4769 MW. While total power consumed was found to be 1.2236 MW compared to base power consumed at 1.699 MW. The weights $a = 1/5$ and $b = 1/2$.

Therefore $L_S = 27.98$, $P_G = 8.04$, and RI = 15.9.

The power density distribution of buses 1, 2, and buses 3, 4, and 5 after load shedding for the IEEE-5 bus system are

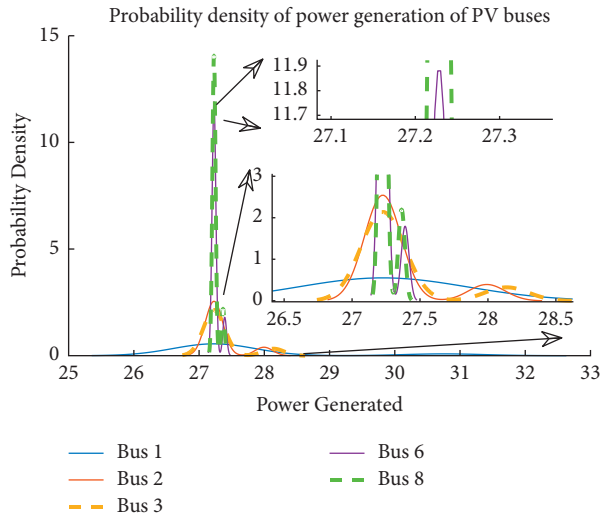

Figure 16: Power density distribution at buses 1, 2, 3, 6, and 8.

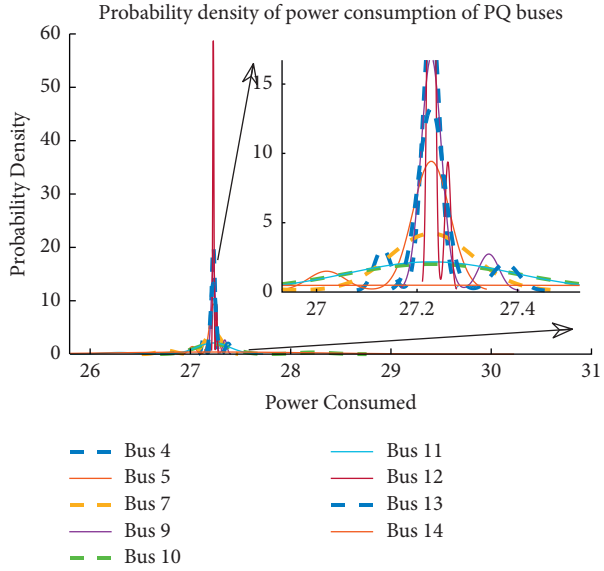

Figure 17: Power density distribution at buses 4, 5, 7, and 9–14.

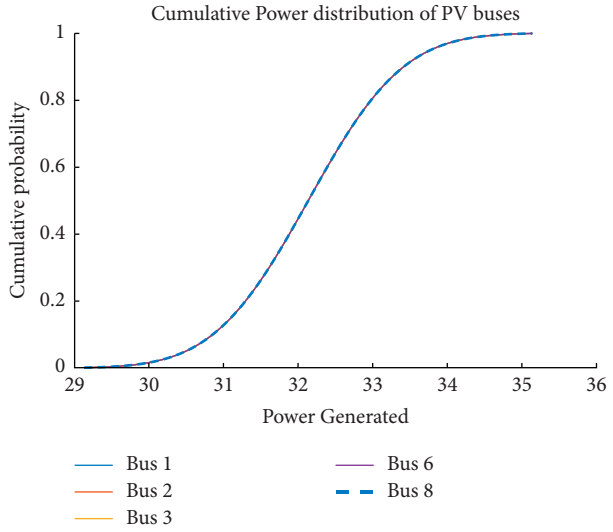

Figure 18: Cumulative power distribution at buses 1, 2, 3, 6, and 8.

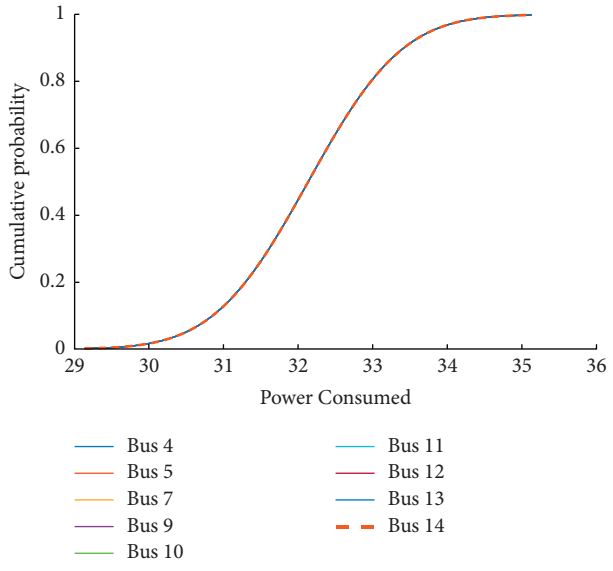

Figure 19: Cumulative power distribution at buses 4, 5, 7, and 9–14.

shown in Figures 12 and 13. Figure 12 shows the slack and generator buses, and Figure 13 shows for load buses.

The commutative power distribution for PV and PQ buses (buses 1–14) before load shedding for the IEEE-14 bus system is shown in Figures 14 and 15.

For the IEEE 14-Bus system without load shedding, the total power generated was found to be 383.0761 MW compared to the base power generation of 35.6310 MW. While total power consumed was found to be 1.9295 MW compared to base power consumed at 2.6922 MW. The weights $a = 1/14$ and $b = 1/11$.

Therefore $L_S = 28.32$, $P_G = 10.75$, and RI = 3.34.

The power density distributions at buses before load shedding for the IEEE-14 bus system are shown in Figures 16 and 17. Figure 16 shows the slack and generator buses, and Figure 17 shows for load buses.

For the IEEE 14-Bus system with load shedding, the total power generated was found to be 383.0761 MW compared to the base power generation of 35.6310 MW. While total power consumed was found to be 1.9295 MW compared to base power consumed at 2.6922 MW. The weights $a = 1/14$ and $b = 1/10$.

Therefore $L_S = 28.32$, $P_G = 10.75$, and RI = 3.59.

The commutative power distribution for PV and PQ buses (buses 1–14) after load shedding for the IEEE-14 bus system is shown in Figures 18 and 19.

The power density distributions at buses after load shedding for the IEEE-14 bus system are shown in Figures 20 and 21. Figure 20 shows the slack and generator buses, and Figure 21 shows for load buses.

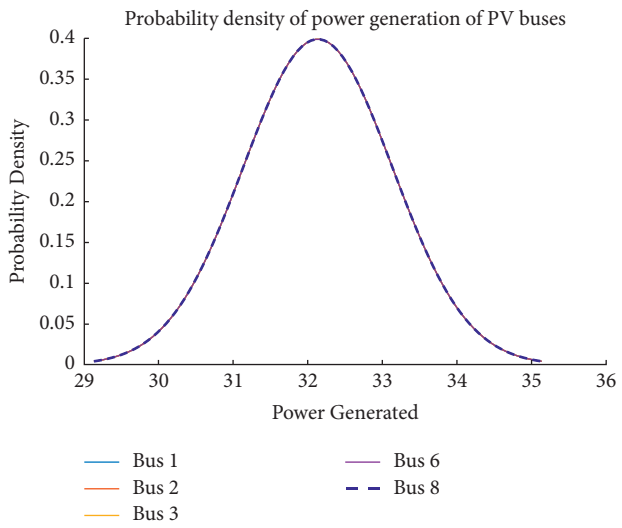

Figure 20: Power density distribution at buses 1, 2, 3, 6, and 8.

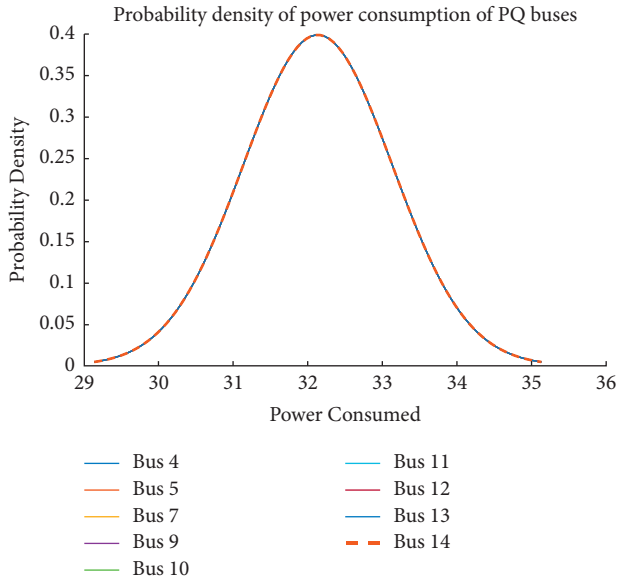

Figure 21: Power density distribution at buses 4, 5, 7, and 9–14.

The comparison between the resilience indices of the systems shows a rise in resilience due to load shedding.

4. Conclusion

The Monte Carlo simulation for the IEEE 5-Bus and IEEE 14-Bus systems, both with and without load shedding, is simulated, and the results are analyzed. The resilience index of both systems reveals that load shedding increases the resilience of the system, as evident from the rate of increase in resilience in each system due to load shedding. The increase in radial lines also causes the simulation to have a higher chance of failure to converge in an NR load flow solution introducing several Not a Number (NaNs) errors. The analysis of the results also reveals that the resilience of a smaller microgrid is larger than the resilience of a larger microgrid. It is also determined that after a certain number of iterations, an increase in the number of iterations does not influence the results of resilience analysis. The open challenge in microgrid resilience is to improve it, and one place to start is by evaluating all possible risks and potential impacts of man-made and natural hazards on the electricity system.

Abbreviations

abrATPG: Average total power generated
ATPC: Average total power consumed
PG: Power generation
LS: Load shedding
pfc: Probability of failure of conductor.

Data Availability

No data were used to support this study.

Conflicts of Interest

The authors declare that they have no conflicts of interest.

References

[1] M. Panteli, C. Pickering, S. Wilkinson, R. Dawson, and P. Mancarella, "Power system resilience to extreme weather: fragility modelling probabilistic impact assessment and adaptation measures," *IEEE Transactions on Power Systems*, vol. 32, no. 5, 2016.

[2] M. Panteli, D. N. Trakas, P. Mancarella, and N. D. Hatziargyriou, "Boosting the power grid resilience to extreme weather events using defensive islanding," *IEEE Transactions on Smart Grid*, vol. 7, p. 6, 2016.

[3] J. Najafi, A. Peiravi, and J. M. Guerrero, "Power distribution system improvement planning under hurricanes based on a new resilience index," *Sustainable Cities and Society*, vol. 39, pp. 592–604, 2018.

[4] H. Gao, Y. Chen, Y. Xu, and C. C. Liu, "Resilience-oriented critical load restoration using microgrids in distribution systems," *IEEE Transactions on Smart Grid*, vol. 7, pp. 2837–2848, 2016.

[5] Y. Xu, C. C. Liu, K. P. Schneider, F. K. Tuffner, and D. T. Ton, "Microgrids for service restoration to critical load in a resilient distribution system," *IEEE Transactions on Smart Grid*, vol. 9, pp. 426–437, 2018.

[6] S. Ma, B. Chen, and Z. Wang, "Resilience enhancement strategy for distribution systems under extreme weather events," *IEEE Transactions on Smart Grid*, vol. 9, pp. 1442–1451, 2018.

[7] H. Farzin, M. Fotuhi-Firuzabad, and M. Moeini-Aghtaie, "Enhancing power system resilience through hierarchical outage management in multi-microgrids," *IEEE Transactions on Smart Grid*, vol. 7, pp. 2869–2879, 2016.

[8] P. Bajpai, S. Chanda, and A. K. Srivastava, "A novel metric to quantify and enable resilient distribution system using Graph theory and Choquet integral," *IEEE Transactions on Smart Grid*, vol. 9, pp. 2918–2929, 2018.

[9] B. Li, R. Roche, and A. Miraoui, "A temporal-spatial natural disaster model for power system resilience improvement

using DG and lines hardening," in *IEEE Conferences IEEE Manchester PowerTech*, Manchester, UK, June 2017.

[10] G. Huang, J. Wang, C. Chen, J. Qi, and C. Guo, "Integration of preventive and emergency responses for power grid resilience enhancement," *IEEE Transactions on Power Systems*, vol. 32, pp. 4451–4463, 2017.

[11] M. Zare-Bahramabadi, A. Abbaspour, M. Fotuhi-Firuzabad, and M. Moeini-Aghtaie, "Resilience-based framework for switch placement problem in power distribution systems," *IET Generation, Transmission & Distribution*, vol. 12, pp. 1223–1230, 2018.

[12] S. Mousavizadeh, M. R. Haghifam, and M. H. Shariatkhah, "A linear two-stage method for resiliency analysis in distribution systems considering renewable energy and demand response resources," *Applied Energy*, vol. 211, pp. 443–460, 2018.

[13] A. Gholami, T. Shekari, F. Aminifar, and M. Shahidehpour, "Microgrid scheduling with uncertainty: the quest for resilience," *IEEE Transactions on Smart Grid*, vol. 7, pp. 2849–2858, 2016.

[14] K. Eshghi, B. K. Johnson, and C. G. Rieger, "Metrics required for power system resilient operations and protection," in *Proceedings of the IEEE Conference*, Eire, PA, USA, October 2016.

[15] S. Chanda and A. K. Srivastava, "Defining and enabling resiliency of electric distribution systems with multiple microgrids," *IEEE Transactions on Smart Grid*, vol. 7, pp. 2859–2868, 2016.

[16] M. Panteli, P. Mancarella, D. N. Trakas, E. Kyriakides, and N. D. Hatziargyriou, "Metrics and quantification of operational and infrastructure resilience in power systems," *IEEE Transactions on Power Systems*, vol. 32, pp. 4732–4742, 2017.

[17] M. Panteli, D. N. Trakas, P. Mancarella, and N. D. Hatziargyriou, "Power systems resilience assessment: hardening and smart operational enhancement strategies," *Proceedings of the IEEE*, vol. 105, pp. 1202–1213, 2017.

[18] Y. Xu, C. Liu, Z. Wang et al., ""DGs for service restoration to critical loads in a secondary network"," *IEEE Transactions on Smart Grid*99 pages, 2018.

[19] A. Singaravelan and M. Kowsalya, "A fuzzy-based approach for microgrids islanded operation," in *Proceedings of the IEEE Conferences 2013 International Conference on Energy Efficient Technologies for Sustainability*, Nagercoil, India, April 2013.

[20] N. Nikmehr, S. Najafi-Ravadanegh, and A. Khodaei, "Probabilistic optimal scheduling of networked microgrids considering time-based demand response programs under uncertainty," *Applied Energy*, vol. 198, pp. 267–279, 2017.

[21] B. Chen, C. Chen, J. Wang, and K. L. Butler-Purry, "Sequential service restoration for unbalanced distribution systems and microgrids," *IEEE Transactions on Power Systems*, vol. 33, pp. 1507–1520, 2018.

[22] H. Ji, C. Wang, P. Li, G. Song, and J. Wu, "SOP-based islanding partition method of active distribution networks considering the characteristics of DG, energy storage system and load," *Energy*, vol. 155, pp. 312–325, 2018.

[23] S. Chanda, A. K. Srivastava, M. U. Mohanpurkar, and R. Hovsapian, "Quantifying power distribution system resiliency using code based metric," *IEEE Transactions on Industry Applications*, vol. 54, pp. 3676–3686, 2018.

[24] C. Chen, J. Wang, F. Qiu, and D. Zhao, "Resilient distribution system by microgrids formation after natural disasters," *IEEE Transactions on Smart Grid*, vol. 7, pp. 958–966, 2016.

[25] M. Panteli and P. Mancarella, "Modeling and evaluating the resilience of critical electrical power infrastructure to extreme weather events," *IEEE Systems Journal*, vol. 11, pp. 1733–1742, 2017.

[26] A. Gholami and F. Aminifar, "A hierarchical response-based approach to the load restoration problem," *IEEE Transactions on Smart Grid*, vol. 8, pp. 1700–1709, 2017.

[27] D. A. Reed, K. C. Kapur, and R. D. Christie, "Methodology for assessing the resilience of networked infrastructure," *IEEE Systems Journal*, vol. 3, pp. 174–180, 2009.

[28] A. Arab, A. Khodaei, S. K. Khator, and Z. Han, "Electric power grid restoration considering disaster economics," *IEEE Access*, vol. 4, 2016.

[29] P. Eder-Neuhauser, T. Zseby, and J. Fabini, "Security: resilience and security: a qualitative survey of urban smart grid architectures," *IEEE Access*, vol. 4, pp. 839–848, 2016.

[30] R. Eskandarpour and A. Khodaei, "Machine learning based power grid outage prediction in response to extreme events," *IEEE Transactions on Power Systems*, vol. 32, pp. 3315-3316, 2017.

[31] L. Liang, Y. Hou, D. J. Hill, and S. Y. R. Hui, "Enhancing resilience of microgrids with electric Springs," *IEEE Transactions on Smart Grid*, vol. 9, p. 1, 2016.

[32] Y. Liu, Q. H. Wu, and X. X. Zhou, "Coordinated multiloop switching control of DFIG for resilience enhancement of wind power penetrated power systems," *IEEE Transactions on Sustainable Energy*, vol. 7, pp. 1089–1099, 2016.

[33] X. Liu, M. Shahidehpour, Z. Li et al., "Microgrids for enhancing the power grid resilience in extreme conditions," *IEEE Transactions on Smart Grid*, vol. 8, no. 2, pp. 589–597, 2016.

[34] S. Mishra, K. Anderson, B. Miller, K. Boyer, and A. Warren, "Microgrid resilience: a holistic approach for assessing threats, identifying vulnerabilities, and designing corresponding mitigation strategies," *Applied Energy*, vol. 264, Article ID 114726, 2020.

[35] J. Duan, H. Li, X. Zhang et al., "A deep reinforcement learning based approach for optimal active power dispatch," in *Proceedings of the 2019 IEEE Sustainable Power and Energy Conference (iSPEC)*, pp. 263–267, Beijing, China, November 2019.

[36] A. Ali, K. Mahmoud, and M. Lehtonen, "Optimal planning of inverter-based renewable energy sources towards autonomous microgrids accommodating electric vehicle charging stations," *IET Generation, Transmission & Distribution*, vol. 16, no. 2, pp. 219–232, 2022.

[37] A. Ali, K. Mahmoud, and M. Lehtonen, "Optimization of photovoltaic and wind generation systems for autonomous microgrids with PEV-parking lots," *IEEE Systems Journal*, vol. 16, no. 2, pp. 3260–3271, 2022.

[38] A. Ali, K. Mahmoud, and M. Lehtonen, "Multiobjective photovoltaic sizing with diverse inverter control schemes in distribution systems hosting EVs," *IEEE Transactions on Industrial Informatics*, vol. 17, no. 9, pp. 5982–5992, 2021.